



Since January 2020 Elsevier has created a COVID-19 resource centre with free information in English and Mandarin on the novel coronavirus COVID-19. The COVID-19 resource centre is hosted on Elsevier Connect, the company's public news and information website.

Elsevier hereby grants permission to make all its COVID-19-related research that is available on the COVID-19 resource centre - including this research content - immediately available in PubMed Central and other publicly funded repositories, such as the WHO COVID database with rights for unrestricted research re-use and analyses in any form or by any means with acknowledgement of the original source. These permissions are granted for free by Elsevier for as long as the COVID-19 resource centre remains active.



Type 2 diabetes mellitus impaired nasal immunity and increased the risk of hyposmia in COVID-19 mild pneumonia patients

Yi Zhao^{a,1}, Yujie Liu^{b,1}, Fangzheng Yi^a, Jun Zhang^c, Zhaohui Xu^{d,*}, Yehai Liu^{a,*}, Ye Tao^{a,*}

^a Department of Otolaryngology-Head and Neck Surgery, The First Affiliated Hospital of Anhui Medical University, Hefei 230022, China

^b Department of Otolaryngology-Head and Neck Surgery, Key Laboratory of Otolaryngology-Head and Neck Surgery, Beijing Tongren Hospital, Capital Medical University, Beijing 100730, China

^c Department of Internal Medicine, University of California at Davis, Davis, 95616, United States

^d Department of Disease Prevention and Control, Xijing 986 Hospital, Fourth Military Medical University, Xi'an 710000, China

ARTICLE INFO

Keywords:

Type 2 diabetes mellitus
COVID-19
Nasal-associated lymphoid tissue
Olfactory dysfunction
Hyposmia

ABSTRACT

In patients with COVID-19, type 2 diabetes mellitus (T2DM) can impair the function of nasal-associated lymphoid tissue (NALT) and result in olfactory dysfunction. Exploring the causative alterations of T2DM within the nasal mucosa and NALT could provide insight into the pathogenic mechanisms and bridge the gap between innate immunity and adaptive immunity for virus clearance. Here, we designed a case-control study to compare the olfactory function (OF) among the groups of normal control (NC), COVID-19 mild pneumonia (MP), and MP patients with T2DM (MPT) after a 6–8 months' recovery, in which MPT had a higher risk of hyposmia than MP and NC. No significant difference was found between the MP and NC. This elevated risk of hyposmia indicated that T2DM increased COVID-19 susceptibility in the nasal cavity with unknown causations. Therefore, we used the T2DM animal model (db/db mice) to evaluate how T2DM increased COVID-19 associated susceptibilities in the nasal mucosa and lymphoid tissues. Db/db mice demonstrated upregulated microvasculature ACE2 expression and significant alterations in lymphocytes component of NALT. Specifically, db/db mice NALT had increased immune-suppressive TCR $\gamma\delta^+$ CD4 $^-$ CD8 $^-$ T and decreased immune-effective CD4 $^+$ /CD8 $^+$ TCR β^+ T cells and decreased mucosa-protective CD19 $^+$ B cells. These results indicated that T2DM could dampen the first-line defense of nasal immunity, and further mechanic studies of metabolic damage and NALT restoration should be one of the highest importance for COVID-19 healing.

1. Introduction

Since December 2019, severe acute respiratory syndrome coronavirus 2 (SARS-CoV-2) infection and coronavirus disease 2019 (COVID-19) has caused a pandemic outbreak in over 200 countries, resulting in millions of confirmed cases of infection worldwide [1]. The underlying diseases, including type 2 diabetes mellitus (T2DM), hypertension, and other diseases that impair the immune system, can not only increase the susceptibility to COVID-19 but also enhance COVID-19 severity and lethality [2,3]. In confirmed cases of COVID-19, olfactory dysfunction (OD) and gustatory dysfunction were the initial syndromes with a high incidence that consistently appeared 2–3 days before the consequent pneumonia syndromes [4,5].

SARS-CoV-2 can attack the olfactory nerves or the mucosal tissue

surrounding them and result in OD [6]. SARS-CoV-2 can use a specific domain structure called spike 1 protein (S1 protein) to bind angiotensin-converting enzyme 2 (ACE2), which is widely expressed on endothelial cells or epithelial cells, particularly on those cells distributed in the microvasculature for metabolic exchange [2,7,8]. Moreover, transmembrane protease serine 2 (TMPRSS2) can facilitate SARS-CoV-2 infection via two independent mechanisms, proteolytic cleavage of the ACE2 receptor, which promotes viral uptake, and cleavage of the S1 glycoprotein, which activates the glycoprotein for host cell entry [9,10].

After cellular entry, SARS-CoV-2 starts to reproduce and results in tissue damage, while the host immune system initiates the specific virus-antigen recognition and presentation process and triggers adaptive immune responses [11]. As the first line of mucosal host defense, nasopharynx-associated lymphoid tissue (NALT) is a tertiary lymphoid

* Corresponding authors.

E-mail addresses: xu231500@163.com (Z. Xu), liyuehai@ahmu.edu.cn (Y. Liu), dmcty@126.com (Y. Tao).

¹ These authors contributed equally to this work.

tissue [12]. NALT can initiate innate immunity, recognize and present specific antigens (via dendritic cells (DCs) and macrophages) and induce T helper 1 (Th1) and T helper 2 (Th2) cells, follicular T helper (T_{FH}) cells, virus-specific cytotoxic $CD8^+$ T lymphocytes (CTLs), and committed B cells [12–14]. Importantly, the specific plasma cells that secrete atopic monoclonal antibodies (e.g., IgM, IgA, and IgG) can neutralize SARS-CoV-2 and thereby cure COVID-19 effectively [15].

The NALT plays a crucial role in the first-line host defense against SARS-CoV-2 and the OD prevention and olfactory function (OF) recovery. However, T2DM can alter NALT, increase disease susceptibility and severity, aggravate OD, and impair the recovery of olfactory function. Furthermore, in COVID-19 pneumonia patients with concomitant T2DM, the risk of OD and the functional alterations of NALT remain unclear. Therefore, our study focused on two areas: (a) assess the joint risk (SARS-CoV-2 and T2DM) on OD in COVID-19 pneumonia patients and (b) use a mouse model to mirror the causative alterations of T2DM associated with COVID-19 susceptibility and delineate their crucial changes (ACE2 and TMPRSS2 entry factors; lymphocyte type and quantity) that might increase the risk of OD in the nasal mucosa and NALT.

2. Materials and methods

2.1. Study design and patient enrollment

This study was designed to evaluate the T2DM-associated risks of OD in COVID-19. For this purpose, we used matched-pair analysis to remove confounding factors effectively and thereby set up three groups, as follows: (1) normal control (NC) healthy subjects for olfactory function baseline evaluation; (2) matched-pair COVID-19 patients with a single diagnosis of mild pneumonia (COVID-19 MP); and (3) COVID-19 patients with a diagnosis of mild pneumonia and T2DM (COVID-19 MPT).

We reviewed the medical records of 1179 consecutive patients (patient database) with a confirmed diagnosis (either nucleic acid positive or antibody positive for SARS-CoV-2 infection and identification via lung CT imaging) in Wuhan Huoshenshan Hospital, Wuhan Union Oncology Hospital, and the First Affiliated Hospital of Anhui Medical University from Jan 18th to Apr 10th, 2020. Since COVID-19 was progressive and associated with many susceptible variants that can impact OF (e.g., hypertension, advanced age, immune state of individuals, smoking history, cancer), we made an inclusion criterion to enroll the patients and an excluding criteria to avoid the interference of those multiple variants in the OF evaluation and analysis (Table 1). Once the case met one condition of the exclusion criteria, that case would be excluded in this study. Eventually, the COVID-19 MPT group had 41 cases available for matching. Additionally, we used C-peptide to discriminate the T1DM (c-peptide ≤ 0.2 nmol/l) and T2DM (C-peptide > 0.2 nmol/l) [16], and glutamate decarboxylase antibody positivity (GADA +) to diagnose the latent autoimmune diabetes in adults (LADA) [17].

We screened the patient database again and collected epidemiologic and clinical information (e.g., age, sex, and treatment) to establish the matched-pair study design (from Jul 18th to Aug 18th). The matched-pair ratio was followed at a 1:1 ratio for both COVID-19 MP and NC group data. The matching criteria were as follows: (1) age difference \leq ten years; (2) same-sex; (3) diagnosis time from disease onset < 1 week; (4) identical therapeutic strategy (e.g., dosage and use time of antibiotics, antiviral drugs, and glucocorticoids); and (5) no significant history of anosmia before November 2019.

Finally, a total of 123 subjects (41 NC, 41 COVID-19 MP, and 41 COVID-19 MPT) were enrolled in this matched-pair analysis for post-healing olfactory function tests, and their clinical characteristics are shown in Supplemental Table 1. In addition, the time-point for testing olfactory function was set up at 6–8 months after the pneumonia healing (from Jul 18th to Oct 1st), and the healing standards were based on repeated negativity of the nucleus acid test (time interval ≥ 72 h) and

Table 1
Inclusion and exclusion criteria for mild pneumonia patients with T2DM.

	Inclusion Criteria	Exclusion Criteria
Population	(1) age range: $36 \leq y \leq 55$ years; (2) MP with repeated CT diagnosis; (3) admitted to hospitals from Jan 18th to Apr 10th, 2020.	(1) severe or critical pneumonia; (2) hypertension; (3) cancer; (4) cardiovascular diseases; (5) healing time more than three weeks; (6) diabetes complications (e.g., peripheral neuropathy, diabetic foot, and nephropathy); (7) history of anosmia or hyposmia before November 2019 (e.g., head trauma, cystic fibrosis); (8) chronic obstructive pulmonary disease (COPD) and other pulmonary diseases; (9) smoking history; (10) other immune deficiency diseases (e.g., autoimmune disease and renal failure); (11) laboratory inspections (e.g., high IL-6 level) that indicated severe disease; (12) chronic sinusitis with CT scan identification; (13) Kallman syndrome; (14) severe allergic rhinitis.
T2DM diagnosis	(1) Patients who were diagnosed with T2DM; (2) newly diagnosed patients with $A1c \geq 6.5\%$, fasting plasma glucose ≥ 7.0 mmol/L, random plasma glucose ≥ 11.1 mmol/L, and symptoms (e.g., polyuria, polydipsia, unintentional weight loss); (3) c-peptide > 0.2 nmol/l.	(1) previously confirmed diagnosis of T1DM; (2) latent autoimmune diabetes in adults (LADA) with Glutamate decarboxylase antibody positivity (GADA +). (3) c-peptide ≤ 0.2 nmol/l.
Chest CT scan	(1) mild type: manifested ground-glass opacities and consolidation, thin and small subpleural patchy, in either single or bilateral lobes.	(1) healthy type: did not exhibit alterations on the pulmonary imaging; (2) progressive type, large lesions and multiple lung lobes that involved in bilateral lungs, accompanied with bronchial retraction, bronchiectasis, and interlobular pleural thickening; and (3) severe type, bilateral lungs exhibited diffused Lesions with uneven distribution of density and large areas of consolidation and ground-glass opacities. Large lesions of the lung resulted in the sign of “white lung,” with or without thickened interlobular pleura, and bilateral pleura and pleural effusion.
Frequency of chest CT scan	Chest CT scan was performed in a time interval of 3–7 days in a stable disease condition.	If the disease progressed rapidly and symptoms exacerbated, the chest CT scan would be performed every day or twice a day.
Healing standard	(1) repeated negativity of COVID-19 nucleic acid test (time interval ≥ 72 h); (2) disappearance of COVID-19 associated symptoms (e.g., fever, cough); (3) Chest CT scan: above mentioned CT manifestations disappeared or became a subpleural thin curvilinear opacity with well-defined edges paralleling the pleural surface.	(1) repeated negativity of COVID-19 nucleic acid test (time interval ≥ 72 h); (2) chest CT scan: large lesions were absorbed, and the formation of widespread ground-glass opacification and considerable architectural distortion; (3) death

chest CT scan diagnosis. All subjects in this study signed an informed consent form, and the institutional review boards (IRBs) of those previously mentioned hospitals approved this study protocol.

2.2. Olfactory function evaluation

Before olfactory function evaluation, we used the anterior rhinoscopy and nasal CT scan to exclude the hyposmia or anosmia caused by severe allergic rhinitis and nasal obstructive diseases (e.g., chronic sinusitis, nasal polyps). We used the test of Sniffin's Sticks for olfactory function evaluation, which could distinguish between normosmics and anosmics in a highly significant manner and had been validated in Chinese population as previously described [18–20]. Briefly, results of the Sniffin's Sticks are presented as composite “threshold-discrimination-identification score” (TDI), the sum of its three independent tests of threshold (T), discrimination (D), and identification (I). Discrimination and identification were scored from 0 to 16, and threshold was scored from 1 to 16, and the total sum of TDI score ranged from 1 to 48, with higher scores reflecting better OF [18,19]. In this study, all enrolled subjects completed the Sniffin's Sticks with an ensured performance of each statement.

2.3. Mouse species and source

The IRB of Anhui Medical University approved this experiment, which was performed in compliance with the national guidelines for the care and use of laboratory animals. In this study, all mice were male mice on the C57BL/6J background at 9–10 weeks old. This study obtained 20 specific pathogen-free (SPF) mice (10 wt and 10 db/db mice) from Nanjing Model Animal Institute, and mice were housed under SPF conditions and sacrificed for sample collection. Precisely, those mice experiments, independent of the smell tests in patients, were executed from May 1st to Jul 18th.

2.4. Pathology sample preparation and IHC and immunofluorescence methods

We used a microscope to ensure the nasal cavity's completeness and removed the covering fur and skin, the bone of the incisors and zygomatic bow and the top partition of the skull and the cerebrum tissue. Tissue fixation, decalcification, embedding, and sectioning were performed according to previously described protocols [21]. In addition, the IHC staining methods and immunofluorescence experiments were used according to previously described protocols [22]. A schematic diagram of the mouse nasal cavity is shown in Supplemental Fig. 1.

2.5. Lymphocyte isolation from NALT

We separated the NALT as previously described [23]. We sacrificed the mice under anesthesia (diethyl ether) via decapitation and removed the lower jaws and tongues. After their removal, we excised the palates and carefully dissected the palates from the bone tissues with fine forceps and a scalpel blade. Furthermore, we placed the palates (including the NALT) in a Petri dish containing ice-cold Hank's balanced salt solution with 5% heat-inactivated fetal bovine serum and gently agitated the NALT on a stainless steel mesh to release the cells. Then, we washed the NALT cell suspension three times and filtered the cell suspension with nylon wool to remove large cellular aggregates.

2.6. Reagents

For IHC staining, we used the following antibodies: anti-ACE2 antibody (ab108252), anti-TMPRSS2 antibody (ab242384) and anti-OMP antibody (ab183947) from Abcam.cn. Furthermore, ServiceBio Company provided the following antibodies: anti-CD19 antibody (GB11061-1); anti-CD45 antibody (GB11066); anti-F4/80 antibody (GB11027);

anti-CD3 antibody (ab16669); anti-CD4 antibody (GB13064-2); anti-CD8 antibody (GB13429); anti-CD11b antibody (GB11058); and anti-CD11c antibody (GB11059).

For flow cytometry, we used the following antibodies: anti-TCR β antibody (FITC, BD 553170); anti-TCR $\gamma\delta$ antibody (PE, BD 553178); anti-CD8a antibody (PP5.5, BD 551162); anti-CD19 antibody (PE-cy7, BD 552854); anti-CD4 antibody (APC-cy7, BD 552051); anti-NK1.1 antibody (BV421, BD 562921); anti-CD45 antibody (BV510, BD 563891); anti-CD11b antibody (PP5.5, BD 550993); anti-CD11c antibody (PE-cy7, BD 558079); anti-F4/80 antibody (APC, BD 566787); and anti-MHCII antibody (APC-cy7, Biolegend 107628).

2.7. Statistical analysis

We used SPSS (IBM SPSS software, version 22.0) for statistical analysis. Paired and unpaired Student's *t*-tests were used for subgroup comparisons. The initial classification of TDI scores defined functional normosmia as a TDI score > 30.75, anosmia as a TDI score \leq 16.5, and hyposmia as a score between these two values [24]. Therefore, we divided the groups (NC, COVID-19PT, and COVID-19 MPT) into subgroups of hyposmia group (16.5 < TDI < 31) and normosmia group (TDI \geq 31) [24,25].

We used binary logistic regression to estimate the OR value for OD based on the above grouping methods. $p < 0.05$ was set as significant. *, $p < 0.05$; **, $p < 0.01$; ***, $p < 0.001$.

3. Results

3.1. Increased risk of hyposmia in COVID-19 mild pneumonia patients with T2DM

Pneumonia of COVID-19 is a rapidly progressive disease, and the speed of that progression varied among different individuals. Therefore, that huge variance required dynamic observation on the pneumonia progression, for which chest CT scan was an appropriate method which had classified COVID-19 pneumonia into four subtypes as follows: healthy, mild, progressive and severe (Table. 1). Contrary to the complicated treatments and various outcomes in progressive and severe subtypes, mild pneumonia patients demonstrated a degree of SARS-CoV-2 susceptibility, and their using drugs and disease course were similar, and this similarity provided feasibility for a case-control study in OF evaluation.

We used the method of Sniffin's Sticks for olfactory function evaluation in all enrolled subjects, and none had found anosmia (TDI \leq 16.3). Further the incidence ratios of hyposmia in groups of NC, COVID-19 MP, and COVID-19 MPT were 4.8%, 9.8%, and 31.7%, respectively. In addition, multiple *t*-tests comparisons showed that the NC group had a significantly higher TDI score than either the COVID-19 MP or COVID-19 MPT group, and the COVID-19 MP group also had a higher TDI score than the COVID-19 MPT group; and the comparison between the NC and COVID-19 MP group did not show significance. Specifically, similar results were also shown in separate comparisons among the sub-scores of threshold, discrimination and identification (Fig. 1A–D).

In risk evaluation, COVID-19 MPT patients had a higher risk of hyposmia compared to the NC subjects, (OR, 9.1; 95% CI, 1.8–43.3), while that risk was not significant in MP patients (OR, 2.1; 95% CI, 0.4–12.2). Furthermore, the MPT group had a higher risk of OD than the MP group (OR, 4.3; 95% CI, 1.3–14.6). Moreover, the risk in all COVID-19 patients (COVID-19 MP + COVID-19 MPT) was also significantly different from that in NC subjects (OR, 5.1; 95% CI, 1.1–23.6; Table. 2). Therefore, the COVID-19 MP patients did not show a higher risk of hyposmia while the COVID-19 MPT had increased the incidence, and this result indicated that T2DM could facilitate SARS-CoV-2 invasiveness in the nasal cavity and potentially hamper the olfactory function recovery, thereby increasing the risk of hyposmia.

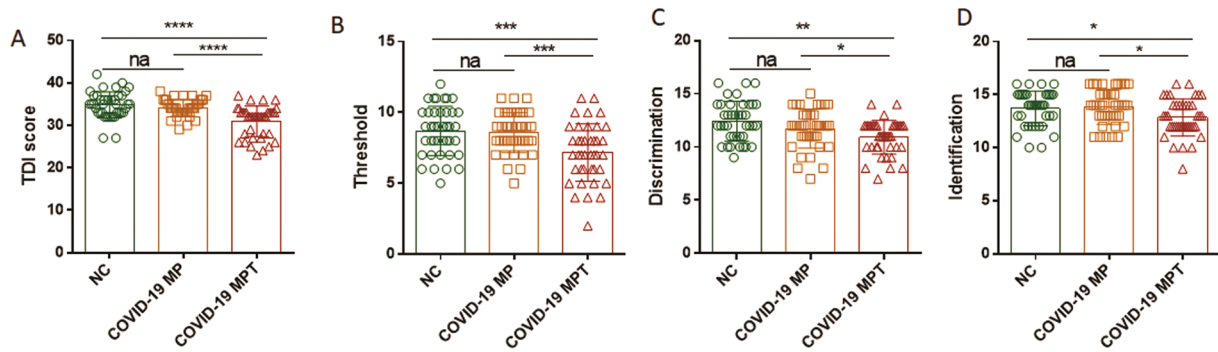


Fig. 1. T2DM increased the risk of OD. (A) multiple *t*-tests comparisons showed that the NC group had a significantly higher TDI score than either the COVID-19 MP or COVID-19 MPT group, and the COVID-19 MP group also had a higher TDI score than the COVID-19 MPT group; and the comparison between the NC and COVID-19 MP group did not show significance. (B-D) similar results were also shown in separate comparisons among the sub-scores of threshold, discrimination and identification, respectively.

Table 2
Risk of hyposmia in COVID-19 mild pneumonia patients.

Risk, Overall vs NC	Risk, MP vs NC	Risk, MPT vs NC	Risk, MPT vs MP
OR 95% CI	OR 95% CI	OR 95% CI	OR 95% CI
5.1 1.1–23.6	2.1 0.4–12.2	9.1 1.8–43.3	4.3 1.3–14.6

NC: normal control.
MP: mild COVID-19 pneumonia.
MPT: mild COVID-19 pneumonia and T2DM.
Overall: MP and MPT.

3.2. Upregulated ACE2 but downregulated TMPRSS2 in the T2DM olfactory mucosa

We used the techniques of tissue decalcification for nasal cavity morphology determination and fluorescence imaging collection, in which the structures of the nasal cavity (e.g., olfactory mucosa, turbinate, and NALT) are shown in Supplemental Fig. 1. The olfactory mucosa of db/db mice had ACE2 upregulation compared to that of wild-type (WT) mouse olfactory mucosa, and ACE2 upregulation was located within the microvasculature that underlies the submucosa (Fig. 2A-F). However, TMPRSS2 was expressed across the olfactory mucosa (mucosal epithelium, lamina propria, and submucosa), and TMPRSS2 expression was decreased in db/db mice, particularly within

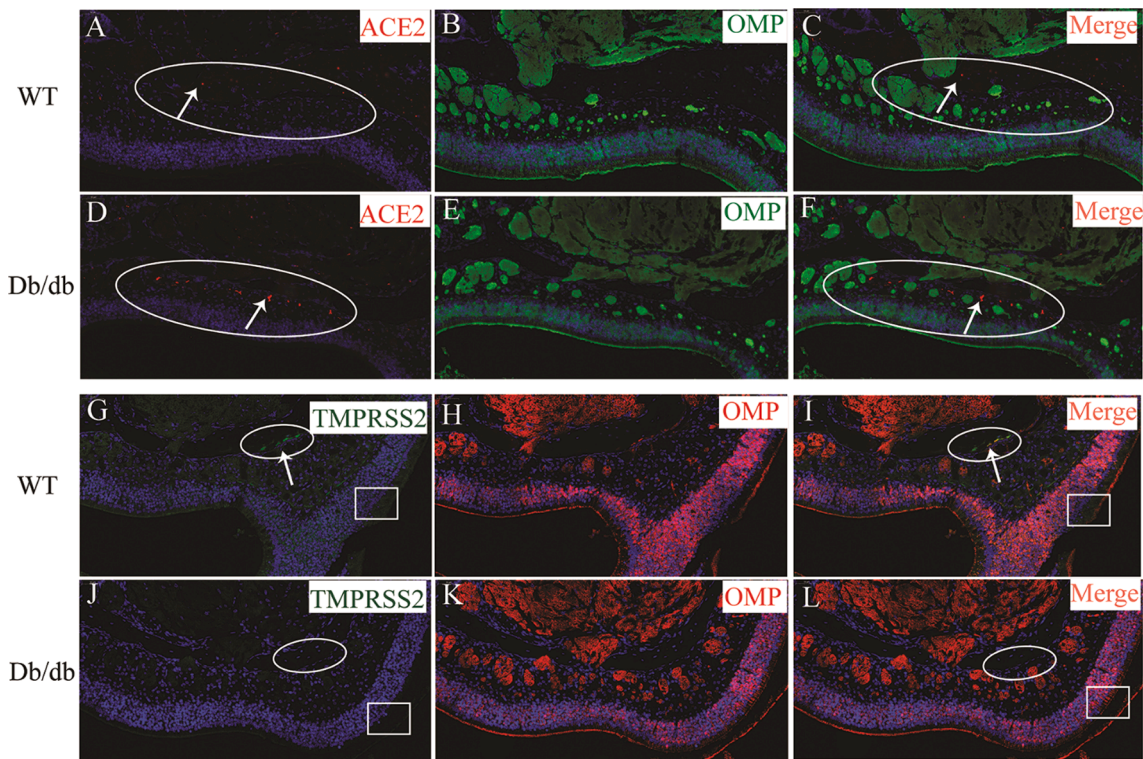


Fig. 2. T2DM upregulated ACE2 expression but decreased TMPRSS2 within the olfactory epithelium. (A-C) and (D-F) show double staining for ACE2 and OMP in the olfactory epithelium of WT and db/db mice, respectively. Db/db mice had higher ACE2 expression than WT mice (oval area, white arrow) within the lamina propria of the olfactory epithelium at the top of the nasal fornix, where olfactory function is highly sensitive. (G-I) and (J-L) show TMPRSS2 double staining in WT and db/db mice, respectively. Db/db mice had lower TMPRSS2 expression than WT mice in both the mucosal epithelium (rectangular area) and lamina propria (white arrow, oval area). (B) and (E) and (H) and (K) show OMP single staining in WT and db/db mice, respectively. The OMP staining intensity showed no significant alterations between the compared groups.

the mucosal epithelium (Fig. 2G-L). These results indicated that T2DM increased the susceptibility to COVID-19, which may be mainly attributed to ACE2 upregulation. In addition, we did not find a significant alteration in olfactory marker protein (OMP) expression (Fig. 2B and 2E; Fig. 2H and 2 K), but the thickness of the olfactory mucosa and the top of the nasal fornix, where olfactory function is highly sensitive, were significantly reduced in db/db mice compared with those in WT control mice ($p < 0.05$; Supplemental Fig. 2A-G). Furthermore, flow cytometry was used to isolate and count the cell number, and the db/db mice had a significant total cell number and CD45⁺ lymphocyte reduction compared to those of the WT control mice (Supplemental Fig. 2H). Therefore, mucosal thinness and cell reduction indicated that T2DM might result in mucosal atrophy and NALT dysfunction, thereby increasing COVID-19 susceptibility and further impairing olfactory nerve regeneration after SARS-CoV-2 insult.

3.3. Increased TCR $\gamma\delta$ ⁺ T cells and decreased TCR β ⁺ T and CD19⁺ B cells in T2DM NALT

Cluster of differentiation 3 (CD3) is a T cell receptor that is expressed on both CD4⁺ and CD8⁺ T cells, and CD19 is a biomarker for normal and neoplastic B cells. Db/db mice showed significant CD3⁺ T and CD19⁺ B cell reduction within NALT compared to those in WT control mice. Furthermore, both CD4⁺ and CD8⁺ lymphocyte counts within NALT were reduced in db/db mice (Fig. 3A-J).

Importantly, a flow cytometry assay demonstrated notable T cell alterations, in which db/db NALT presented increased TCR $\gamma\delta$ ⁺ T cell levels (ratio and quantity) and a decreased quantity of TCR β ⁺CD4⁺ and TCR β ⁺CD8⁺ T cells. In addition, most of the additional TCR $\gamma\delta$ ⁺ T cells were CD4⁺CD8⁻ T cells (99.3%; gating strategies in Supplemental Fig. 3). Furthermore, both the ratio and the quantity of B cells were significantly reduced in NALT (Fig. 3M and 3 N).

3.4. The ratio and quantity of macrophages and DCs in NALT

Macrophages and DCs are innate immune cells that perform an antigen-presenting function that bridges the gap between innate and adaptive immunity. For the marking and positioning of macrophages

and DCs, we used single staining of F4/80 and double staining of CD11b and CD11c. However, we found a few macrophages and DCs within NALT via immunohistochemistry (IHC) fluorescent staining (Fig. 4A-L). Moreover, we also used the flow cytometry assay for gating macrophages and DCs (Supplemental Fig. 4), and their ratios of CD45⁺ leukocytes and overall numbers did not show significant differences (Fig. 4M and 4 N).

4. Discussion

The olfactory mucosal epithelium is the first line of defense against invading respiratory and neurotropic viruses, and the degree of OD may indicate the damage caused by either virus invasiveness or extended host inflammation. Since many underlying diseases and their comorbidities can prolong disease progression and impact quality of life (QOL), we used matched-pair methods to exclude heterozygous factors and thereby evaluate the associated risk of T2DM in SARS-CoV-2-caused OD. In this case-control study, we enrolled 123 subjects (NC, $n = 41$; COVID-19 MP $n = 41$; and COVID-19 MPT), and the incidence ratios of hyposmia in the NC, COVID-19 MP, and COVID-19 MPT groups were 4.8%, 9.8%, and 31.7%, respectively. Specifically, COVID-19 MPT patients had an increased risk of hyposmia (MPT vs. MP, OR: 4.3, [95% CI, 1.3–14.6]; MPT vs. NC, OR: 9.1, [95% CI, 1.8–43.3]). Notably, the db/db mouse model reflecting COVID-19 susceptibility showed two potential mechanisms in T2DM-associated risk of OD, as follows: (1) upregulated ACE2 expression in the microvasculature of the lamina propria; (2) nasal immunity deficiency via NALT lymphocyte reduction (CD4⁺ and CD8⁺ T cells and CD19⁺B cells).

Upregulation of ACE2 is a compensatory mechanism in T2DM but facilitates SARS-CoV-2 entry, and the location of ACE2 upregulation in the nasal cavity indicated the first site where the virus initiates colonization and replication. Functionally, ACE2 can transform angiotensin II into angiotensin (Ang 1–7), and Ang1-7 can oppose the effects of AngII and thereby negatively regulate the renin-angiotensin (RAS) system [2,7,8,26]. In T2DM and hypertension, particularly in patients those treated with ACE inhibitors and angiotensin II type I receptor blockers (ARBs), ACE2 expression is substantially upregulated for cardiovascular homeostasis maintenance [2], and this upregulation facilitates the entry

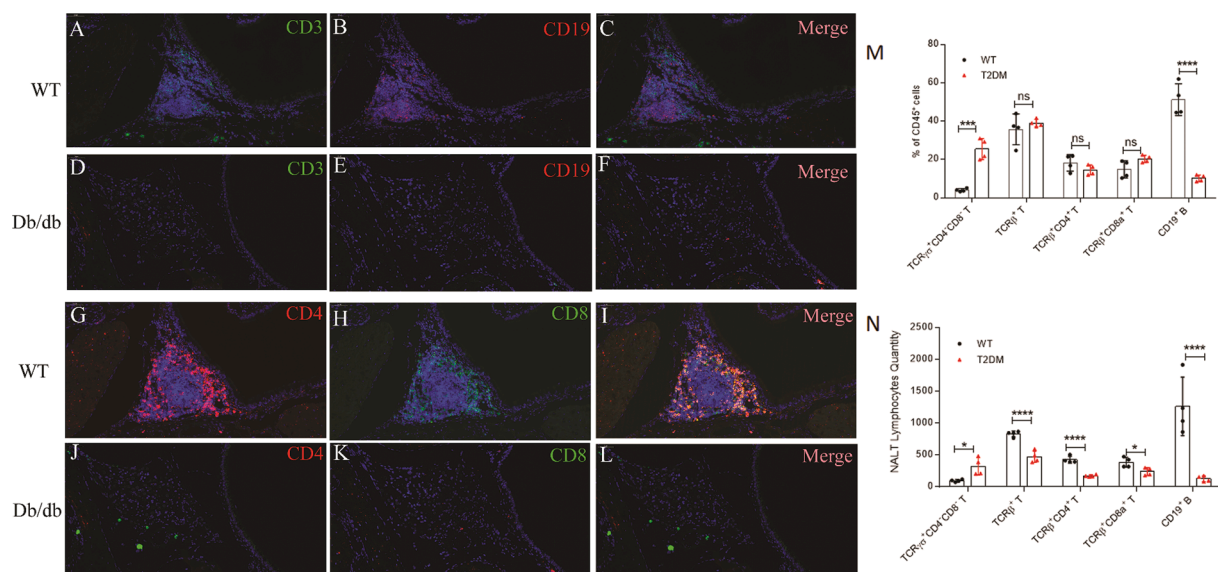


Fig. 3. T2DM resulted in T and B cell deficiency in NALT. (A-C) and (D-F) show CD3 and CD19 double staining, and db/db mice showed a significant reduction in CD3⁺ T cells and CD19⁺ B cells in NALT. (G-I) and (J-L) show CD4 and CD8 double staining in WT and db/db mice, respectively; compared to WT, db/db mice had a significant reduction in both CD4⁺ and CD8⁺ T lymphocytes in NALT. (M) and (N) show the ratio and quantity of CD45⁺ lymphocytes, respectively. (M) Db/db NALT showed a significant increase in the CD45⁺ lymphocyte ratio among TCR $\gamma\delta$ ⁺ CD4-CD8⁻ T cells and a notable decrease in the CD45⁺ lymphocyte ratio among CD19⁺ B cells. (N) Db/db NALT demonstrated a significant increase in CD45⁺ lymphocyte quantity among TCR $\gamma\delta$ ⁺ CD4-CD8⁻ T cells and a decrease in the quantity of TCR β ⁺ T, TCR β ⁺ CD4⁺ T, TCR β ⁺ CD8⁺ T, and CD19⁺ B cells (*, $p < 0.05$; ***, $p < 0.001$; ****, $p < 0.0001$).

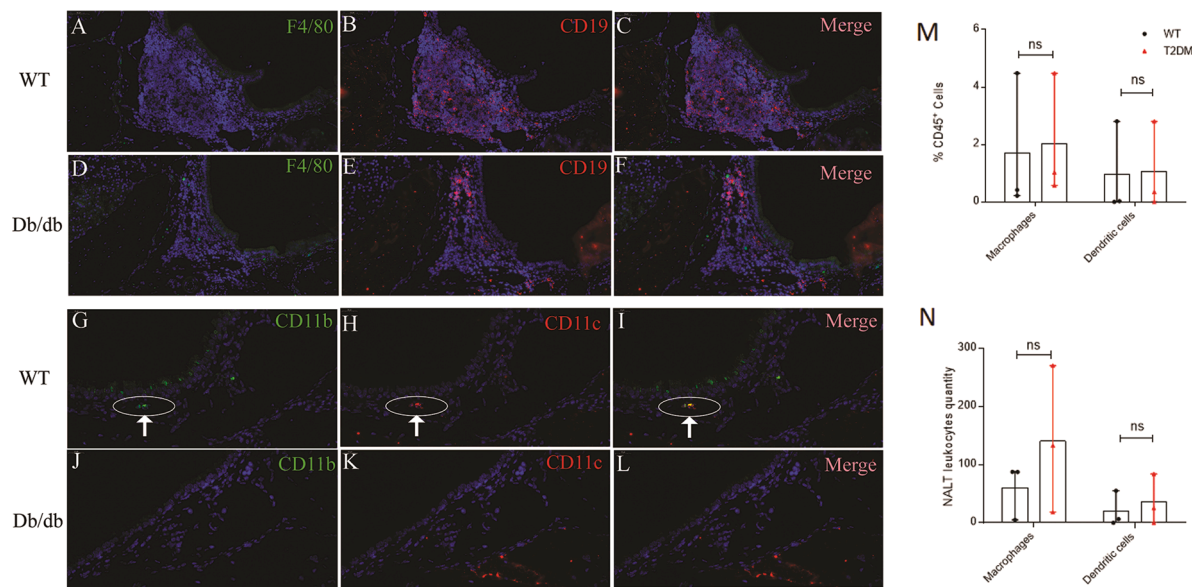


Fig. 4. T2DM did not alter the ratio and quantity of macrophages and DCs in NALT. (A-C) and (D-F) show F4/80 and CD19 double staining for macrophages and B cells in WT and db/db NALT, respectively; WT NALT did not show F4/80 positive staining, and only a few F4/80 positive macrophages were found in db/db NALT. (G-I) and (J-L) show CD11b + CD11c + DCs; we found CD11b + CD11c + double-positive cells near WT NALT, while db/db NALT did not show positive double staining. (M) and (N) show the data from a flow cytometry assay gating macrophages and DCs, and their ratio of CD45 + lymphocytes and overall quantity was low and did not show significant differences between the WT and db/db mice.

of SARS-CoV-2 [27]. Moreover, ACE2 upregulation occurs on the endothelial cells of the microvasculature that are supported and accompanied by olfactory nerve fibers in the olfactory mucosa. Therefore, SARS-CoV-2 causes apoptosis or necrosis of endothelial cells [28] and may impair the blood supply and cause hypoxic ischemia of olfactory fibers [29], thereby resulting in hyposmia [30].

T2DM decreased TMPRSS2 expression and caused mucosal atrophy with thinned olfactory mucosa and epithelium ciliary dysfunction in db/db mice. TMPRSS2 is a plasma membrane-anchored serine protease that participates in proteolytic cascades and maintains prostate homeostasis via the regulation of androgen [31], while TMPRSS2-deficient mice do not show a specific phenotype in survival, breeding, or diseases [32]. Although TMPRSS2 is an entry factor of SARS-CoV-2 and decreased TMPRSS2 expression thereby plays a protective role [33], the mucosal epithelium still expresses sufficient TMPRSS2 to facilitate virus entry. In addition, mucosal atrophy might impair the immune response and hamper olfactory nerve regeneration. Furthermore, contrary to a previous study showing that TMPRSS2 was expressed only within ACE2⁺ cells [27], we found that TMPRSS2 was widely expressed (epithelium mucosa, submucosa and bone marrow) and did not have specific colocalization with ACE2 staining. This finding was consistent with the stratified analysis of ACE2 and TMPRSS2 expression in the nasal olfactory mucosa [34]. Specifically, TMPRSS2 downregulation might be associated with epithelial ciliary dysfunction.

T2DM-induced CD4⁺ and CD8⁺ T cell reduction in NALT might be a crucial factor in immune deficiency that can increase COVID-19 susceptibility and severity and risk of OD. NALT includes all of the immune components for antigen-specific T or B cell-mediated responses, which are necessary for the generation of trained mucosal immunity through the inhalation and presentation of antigens in the respiratory tract [13]. Importantly, innate immunity is the first line of antiviral defense, in which macrophages and DCs capture and internalize virus-specific antigens for presentation to T cells at secondary or tertiary lymphoid organs [35]. In addition, rapid migration of maturing DCs from the mucosal site of infection to NALT is critical for rapid priming of naïve T maturation and B cell activation [36]; those naïve T cells differentiate into antigen-specific effector T cells, and their enrichment can exert effects at sites of virus infection [37]. Functionally, CD4⁺ Th1 cells can

amplify the immune response through classical activation of macrophages and secretion of interferon (IFN)- γ [38], CD4⁺ Th2 cells account for the generation of antigen-specific IgA-producing cells in NALT [39], and coronavirus-specific CD8⁺ CTLs can generate high levels of effective cytokines (IFN- γ and TNF- α) and cytotoxic molecules (perforin and granzyme B) [40].

Furthermore, most $\gamma\delta$ T cells are CD4 and CD8 negative, and they perform a negative immune regulation function that includes tolerance maintenance and hyporesponsiveness to tumors; increased $\gamma\delta$ T cells can inhibit CD8⁺ T cells in HBV-specific responses [41]. Although the underlying mechanisms by which T2DM can increase TCR $\gamma\delta$ ⁺ T cell levels and decrease the TCR β ⁺ T quantity and ratio within NALT remain unclear, inhibited NALT function results in first-line immune deficiency that prolongs the process of the adaptive immune response in COVID-19 and uncontrolled virus infection in the olfactory mucosa, which is further associated with hyposmia.

B cell reduction in NALT devastates the nasal immune response. Most B cells within NALT are naïve B cells (sIgM⁺IgD⁺ phenotype), and they require antigen-presenting cells (APCs) (e.g., DCs, macrophages and T cells) to differentiate them into committed B cells for a specific antiviral immune response. Notably, antigen-specific T_{FH} cells express the surface protein CD40L, which can bind CD40 on B cells, thereby helping B cell activation in a T cell-dependent (TD) manner [42], and antibodies generated via TD B cell activation have a higher affinity than those generated via T cell-independent B cell activation [43]. Therefore, a reduction in B cell quantity and impairment of B cell development could result in deficiencies in antibody production for SARS-CoV-2 clearance, and failed clearance within the olfactory mucosa may result in hyposmia and cerebral infection [44].

Many studies have focused on the entry factors and immune susceptibility risks of SARS-CoV-2 infection; however, the crucial process by which APCs (e.g., macrophages, DCs, and T cells) bridge the gap between innate and adaptive immunity remains mostly unknown [45]. In our study, since SARS-CoV-2 research requires a high standard of control (biosafety level 4), we cannot assess the dynamic progress within a mouse model of virus infection due to limited conditions. Therefore, further explorations on how SARS-CoV-2 damages the olfactory mucosa and how host APCs train naïve T cells into effective T cells and switch B

cells into committed B cells that secrete antibodies to neutralize the virus are essential. In addition, our limited sample size may cause a possible selection bias that could confound the olfactory function results in this study; therefore, additional larger population or functional studies are warranted for validation.

Our results suggested that T2DM resulted in an increased risk of hyposmia in COVID-19, and a T2DM mouse model showed that this increased risk might contribute to elevated ACE2 expression within the microvasculature of the olfactory mucosa and immune deficiency in NALT (T and B cell reduction). Specifically, db/db mice demonstrated an increase in TCR $\gamma\delta^+$ CD4 $^-$ CD8 $^-$ T cell levels and a decrease in TCR β^+ T cell levels (CD4 $^+$ or CD8 $^+$), and TCR $\gamma\delta$ CD4 $^-$ CD8 $^-$ T cells suppressed CD8 $^+$ -mediated antiviral immune responses. Furthermore, the B cell levels also showed a significant reduction in db/db NALT. Therefore, increased immune-suppressive TCR $\gamma\delta^+$ T cell levels and decreased immune-effective TCR β^+ T cell levels, combined with B cell reduction, could represent the immune deficiency state in db/db NALT. NALT is the first line of antiviral defense, and NALT dysfunction can impair B cell development and efficient antibody production for SARS-CoV-2 clearance. Therefore, functional restoration of NALT, which can build the core center in trained immunity, may shed light on the unknown mechanisms within the antigen presentation process and improve the effects of nasal vaccination, thereby improving the prognosis and recovery of olfactory function in COVID-19.

Declaration of Competing Interest

The authors declare that they have no known competing financial interests or personal relationships that could have appeared to influence the work reported in this paper.

Acknowledgments

The authors gratefully thank Ms. Ying Li for laboratory support.

Funding

The China Postdoctoral Science Foundation (2019M652215), the initial research fund of the First Affiliated Hospital of Anhui Medical University, the Fundamental Research Funds for the Central Universities (WK2070000149), the new Medicine Fund of the University of Science and Technology of China (WK2070000170), and the Natural Science Research Project of Anhui Higher Education Institution (grant number: KJ2018ZD021) supported this work.

Author contributions

Y. Z.: study design and manuscript writing; Yujie L.: data collection and analysis; Fangzheng, Y.: data collection and sample preparation; Jun Z.: study design; Zhaohui X.: data collection and clinical study design; Yehai L.: study design; and Ye T.: study design and manuscript editing.

Appendix A. Supplementary data

Supplementary data to this article can be found online at <https://doi.org/10.1016/j.intimp.2021.107406>.

References

- C. Huang, Y. Wang, X. Li, L. Ren, J. Zhao, Y. Hu, L. Zhang, G. Fan, J. Xu, X. Gu, Clinical features of patients infected with 2019 novel coronavirus in Wuhan China, *The Lancet* 395 (10223) (2020) 497–506.
- L. Fang, G. Karakiulakis, M. Roth, Are patients with hypertension and diabetes mellitus at increased risk for COVID-19 infection? *The Lancet. Respiratory Medicine* 8 (4) (2020), e21.
- Y.-Y. Zheng, Y.-T. Ma, J.-Y. Zhang, X. Xie, COVID-19 and the cardiovascular system, *Nature Reviews Cardiology* 17 (5) (2020) 259–260.
- J.R. Lechien, C.M. Chiesa-Estomba, D.R. De Siati, M. Horoi, S.D. Le Bon, A. Rodriguez, D. Dequanter, S. Blecic, F. El Afia, L. Distinguin, Y. Chekkoury-Iddrisi, S. Hans, I.L. Delgado, C. Calvo-Henriquez, P. Lavigne, C. Falanga, M. R. Barillari, G. Cammaroto, M. Khalife, P. Leich, C. Souchay, C. Rossi, F. Journe, J. Hsieh, M. Edjlali, R. Carlier, L. Ris, A. Lovato, C. De Filippis, F. Coppee, N. Fakhry, T. Ayad, S. Saussez, Olfactory and gustatory dysfunctions as a clinical presentation of mild-to-moderate forms of the coronavirus disease (COVID-19): a multicenter European study, *Eur Arch Otorhinolaryngol* (2020).
- S.H.R. Bagheri, A.M. Asghari, M. Farhadi, A.R. Shamshiri, A. Kabir, S.K. Kamrava, M. Jaleesi, A. Mohebbi, R. Alizadeh, A.A. Honarmand, Coincidence of COVID-19 epidemic and olfactory dysfunction outbreak, *Medrxiv* (2020).
- B. Jafek, D. Hartman, P. Eller, E. Johnson, R. Strahan, D. Moran, Postviral olfactory dysfunction, *Am. J. Rhinology* 4 (3) (1990) 91–100.
- I. Hamming, M.E. Cooper, B.L. Haagmans, N.M. Hooper, R. Korstanje, A. D. Osterhaus, W. Timens, A.J. Turner, G. Navis, H. van Goor, The emerging role of ACE2 in physiology and disease, *J Pathol* 212 (1) (2007) 1–11.
- H. Cheng, Y. Wang, G.Q. Wang, Organ-protective effect of angiotensin-converting enzyme 2 and its effect on the prognosis of COVID-19, *J. Med. Virol.* (2020).
- A. Heurich, H. Hofmann-Winkler, S. Gierer, T. Liepold, O. Jahn, S. Pöhlmann, TMPRSS2 and ADAM17 cleave ACE2 differentially and only proteolysis by TMPRSS2 augments entry driven by the severe acute respiratory syndrome coronavirus spike protein, *J. Virology* 88 (2) (2014) 1293–1307.
- M. Hoffmann, H. Kleine-Weber, S. Schroeder, N. Krüger, T. Herrler, S. Erichsen, T. S. Schiergens, G. Herrler, N.-H. Wu, A. Nitsche, SARS-CoV-2 cell entry depends on ACE2 and TMPRSS2 and is blocked by a clinically proven protease inhibitor, *Cell* (2020).
- H. Li, L. Liu, D. Zhang, J. Xu, H. Dai, N. Tang, X. Su, B. Cao, SARS-CoV-2 and viral sepsis: observations and hypotheses, *The Lancet* (2020).
- L. Tacchi, R. Musharrafieh, E.T. Larragoite, K. Crossey, E.B. Erhardt, S.A.M. Martin, S.E. LaPatra, I. Salinas, Nasal immunity is an ancient arm of the mucosal immune system of vertebrates, *Nat. Commun.* 5 (2014) 5205.
- H. Kiyono, S. Fukuyama, NALT- versus Peyer's-patch-mediated mucosal immunity, *Nat. Rev. Immunol.* 4 (9) (2004) 699–710.
- A. Pizzolla, Z. Wang, J.R. Groom, K. Kedzierska, A.G. Brooks, P.C. Reading, L. M. Wakim, Nasal-associated lymphoid tissues (NALTs) support the recall but not priming of influenza virus-specific cytotoxic T cells, *Proc. Natl. Acad. Sci. USA* 114 (20) (2017) 5225–5230.
- C. Wang, W. Li, D. Drabek, N.M. Okba, R. van Haperen, A.D. Osterhaus, F.J. van Kuppeveld, B.L. Haagmans, F. Grosveld, B.-J. Bosch, A human monoclonal antibody blocking SARS-CoV-2 infection, *Nat. Communications* 11 (1) (2020) 1–6.
- E. Leighton, C.A. Sainsbury, G.C. Jones, A practical review of C-peptide testing in diabetes, *Diabetes therapy* 8 (3) (2017) 475–487.
- P.W.S. Rosário, J.S. Reis, T.A. Fagundes, M.R. Calsolari, R. Amim, S.C. Silva, S. Purisch, Latent autoimmune diabetes in adults (LADA): usefulness of anti-GAD antibody titers and benefit of early insulinization, *Arquivos Brasileiros de Endocrinologia Metabologia* 51 (1) (2007) 52–58.
- T. Hummel, K. Kobal, G. Gudziol, H. Mackay-Sim, A. 2007 normative data for the "Sniffin' Sticks" including tests of odor identification, odor discrimination, and olfactory thresholds: an upgrade based on a group of more than 3,000 subjects, *Eur Arch Otorhinolaryngol* 264 237–243.
- T. Hummel, B. Sekinger, S.R. Wolf, E. Pauli, G. Kobal, 'Sniffin' sticks': olfactory performance assessed by the combined testing of odor identification, odor discrimination and olfactory threshold, *Chemical senses* 22 (1) (1997) 39–52.
- G. Chen, H. Pan, L. Li, J. Wang, D. Zhang, Z. Wu, Olfactory assessment in the Chinese pediatric population, *Medicine* 97 (16) (2018).
- S. Shi, C. Cote, K. Kalra, C. Taylor, A. Tandon, A technique for retrieving antigens in formalin-fixed, routinely acid-decalcified, celluloid-embedded human temporal bone sections for immunohistochemistry, *J. Histochemistry Cytochemistry* 40 (6) (1992) 787–792.
- R. Curran, J. Gregory, Demonstration of immunoglobulin in cryostat and paraffin sections of human tonsil by immunofluorescence and immunoperoxidase techniques. Effects of processing on immunohistochemical performance of tissues and on the use of proteolytic enzymes to unmask antigens in sections, *J. Clinical Pathology* 31 (10) (1978) 974–983.
- G.A. Sosa, M.F. Quiroga, M.E. Roux, Flow cytometric analysis of T-lymphocytes from nasopharynx-associated lymphoid tissue (NALT) in a model of secondary immunodeficiency in Wistar rats, *Immunobiology* 214 (5) (2009) 384–391.
- A. Oleszkiewicz, V. Schriever, I. Croy, A. Hähner, T. Hummel, Updated Sniffin' Sticks normative data based on an extended sample of 9139 subjects, *European Archives of Oto-Rhino-Laryngology* 276 (3) (2019) 719–728.
- J.L. Mattos, R.J. Schlosser, K.A. Storck, Z.M. Soler, Understanding the relationship between olfactory-specific quality of life, objective olfactory loss, and patient factors in chronic rhinosinusitis, *Wiley Online Library, International forum of allergy & rhinology*, 2017, pp. 734–740.
- F.J. Warner, J.L. Guy, D.W. Lambert, N.M. Hooper, A.J. Turner, Angiotensin Converting Enzyme-2 (ACE2) and its Possible Roles in Hypertension, *Diab. Cardiac Function* 10 (5) (2003) 377–385.
- W. Sungnak, N. Huang, C. Bécavin, M. Berg, R. Queen, M. Litvinukova, C. Talavera-López, H. Maatz, D. Reichart, F. Sampaziotis, K.B. Worlock, M. Yoshida, J. L. Barnes, SARS-CoV-2 entry factors are highly expressed in nasal epithelial cells together with innate immune genes, *Nature Medicine* 26 (5) (2020) 681–687.
- Z. Varga, A.J. Flammer, P. Steiger, M. Haberecker, R. Andermatt, A.S. Zinkernagel, M.R. Mehra, R.A. Schuepbach, F. Ruschitzka, H. Moch, Endothelial cell infection and endotheliitis in COVID-19, *The Lancet* 395 (10234) (2020) 1417–1418.

- [29] R. Bonfanti, T. Musumeci, C. Russo, R. Pellitteri, The protective effect of curcumin in Olfactory Ensheathing Cells exposed to hypoxia, *European J. Pharmacology* 796 (2017) 62–68.
- [30] A. Drobyshevsky, A.M. Robinson, M. Derrick, A.M. Wyrwicz, X. Ji, I. Englof, S. Tan, Sensory deficits and olfactory system injury detected by novel application of MEMRI in newborn rabbit after antenatal hypoxia–ischemia, *Neuroimage* 32 (3) (2006) 1106–1112.
- [31] B. Lin, C. Ferguson, J.T. White, S. Wang, R. Vessella, L.D. True, L. Hood, P. S. Nelson, Prostate-localized and androgen-regulated expression of the membrane-bound serine protease TMPRSS2, *Cancer research* 59 (17) (1999) 4180–4184.
- [32] T.S. Kim, C. Heinlein, R.C. Hackman, P.S. Nelson, Phenotypic analysis of mice lacking the *Tmprss2*-encoded protease, *Molecular Cellular Biology* 26 (3) (2006) 965–975.
- [33] J.J. Lee, S. Kopetz, E. Vilar, J.P. Shen, K. Chen, A. Maitra, Relative Abundance of SARS-CoV-2 Entry Genes in the Enterocytes of the Lower Gastrointestinal Tract, *Genes* 11 (6) (2020) 645.
- [34] L. Fodouljian, J. Tuberosa, D. Rossier, M. Boillat, C. Kan, V. Pauli, K. Egervari, J.A. Lobrinus, B.N. Landis, A. Carleton, I. Rodriguez, SARS-CoV-2 receptor and entry genes are expressed by sustentacular cells in the human olfactory neuroepithelium, (2020).
- [35] C.E. Hughes, R.A. Benson, M. Bedaj, P. Maffia, Antigen-Presenting Cells and Antigen Presentation in Tertiary Lymphoid Organs, *Front. Immunology* 7 (2016).
- [36] H. Lee, D. Ruane, K. Law, Y. Ho, A. Garg, A. Rahman, D. Esterházy, C. Cheong, E. Goljo, A.G. Sikora, Phenotype and function of nasal dendritic cells, *Mucosal Immunology* 8 (5) (2015) 1083–1098.
- [37] J. Sprent, C.D. Surh, T cell memory, *Annual Rev. Immunology* 20 (1) (2002) 551–579.
- [38] K. Schroder, P.J. Hertzog, T. Ravasi, D.A. Hume, Interferon- γ : an overview of signals, mechanisms and functions, *J. Leukocyte Biol.* 75 (2) (2004) 163–189.
- [39] M. Yanagita, T. Hiroi, N. Kitagaki, S. Hamada, H.-O. Ito, H. Shimauchi, S. Murakami, H. Okada, H. Kiyono, Nasopharyngeal-associated lymphoreticular tissue (NALT) immunity: fimbriae-specific Th1 and Th2 cell-regulated IgA responses for the inhibition of bacterial attachment to epithelial cells and subsequent inflammatory cytokine production, *J. Immunology* 162 (6) (1999) 3559–3565.
- [40] R. Channappanavar, J. Zhao, S. Perlman, T cell-mediated immune response to respiratory coronaviruses, *Immunologic Res.* 59 (1–3) (2014) 118–128.
- [41] Q. Lai, S. Ma, J. Ge, Z. Huang, X. Huang, X. Jiang, Y. Li, M. Zhang, X. Zhang, J. Sun, TCR $\gamma\delta$ + CD4– CD8– T Cells Suppress the CD8+ T-Cell Response to Hepatitis B Virus Peptides, and Are Associated with Viral Control in Chronic Hepatitis B, *PLoS one* 9 (2) (2014) e88475.
- [42] M.D. Cooper, The early history of B cells, *Nature Reviews Immunology* 15 (3) (2015) 191–197.
- [43] S. Crotty, A brief history of T cell help to B cells, *Nature Reviews Immunology* 15 (3) (2015) 185–189.
- [44] A. Paniz-Mondolfi, C. Bryce, Z. Grimes, R.E. Gordon, J. Reidy, J. Lednický, E. M. Sordillo, M. Fowkes, Central nervous system involvement by severe acute respiratory syndrome coronavirus-2 (SARS-CoV-2), *J. Medical Virology* 92 (7) (2020) 699–702.
- [45] M.G. Netea, E.J. Giamarellos-Bourboulis, J. Domínguez-Andrés, N. Curtis, R. van Crevel, F.L. van de Veerdonk, M. Bonten, Trained Immunity: a Tool for Reducing Susceptibility to and the Severity of SARS-CoV-2 Infection, *Cell* (2020).